Correlation between electrical conductivity, viscosity, and structure in borosilicate glass-forming melts

A. Grandjean,[1,*] M. Malki,[2,3] C. Simonnet,[4] D. Manara,[1] and B. Penelon[1]

[1]*CEA-VALRHO, Service de Confinement des Déchets et Vitrification, 30207 Bagnols Sur Cèze, France*
[2]*CNRS-CRMHT, 1D Av de la Recherche Scientifique, 45071 Orléans Cedex 2, France*
[3]*Polytech'Orléans, Université d'Orléans, 8 rue Léonard de Vinci, 45072 Orléans Cedex 2, France*
[4]*Department of Physics, University of California, San Diego, 9500 Gilman Drive, La Jolla, California 92093, USA*

The electrical conductivity and viscosity of borosilicate glass-forming melts were studied over a wide composition and temperature range above the transition temperature T_g. High-temperature Raman spectroscopy was used to characterize the structure of both molten and glassy states of the system. The temperature dependence of both electrical conductivity and viscosity are well described by a Vogel-Fulcher-Tammann (VFT) law. Contrary to the solid state, it appears that in the molten state the boron coordination number is no longer the relevant parameter to account for the compositional dependence of both the electrical conductivity and the viscosity. Our results reveal an interdependence of the electrical conductivity and viscosity with a nonlinear character of the Stokes-Einstein law. This could be explained by a difference in the elementary mechanism of transport between these two properties.

PACS number(s): 61.43.Fs, 66.10.−x, 66.20.+d

I. INTRODUCTION

Borosilicate glasses based on the SiO_2-B_2O_3-Na_2O ternary system are currently the most widely employed glasses for nuclear waste immobilization.[1] They are also widely used for applications ranging from chemically resistant laboratory glassware to optical and sealing glasses. Determining the transport properties of these glass-forming melts is of great importance for a proper understanding of melting processes. Ionic conductivity and viscosity in particular are essential properties for the design and control of Joule-effect industrial melters.

The innovative aspect of this work is that it demonstrates that the effect of the structure on the transport properties differs between the solid and molten states. It also provides a quantitative comparison of the viscosity and conductivity at high temperatures and demonstrates the existence of a simple relation between these properties in oxide melts, depending essentially on diffusing cations.

This paper describes the ionic conductivity and viscosity of glass-forming melts in the SiO_2-B_2O_3-Na_2O (SBN) ternary system over a wide composition range. Viscosity studies in borosilicate melts have previously been reported,[2] but most have dealt with specific compositions, phase-separated glasses,[3,4] have concerned multicomponent borosilicate glasses,[5] or have been carried out in the glass transition region.[6,7] Electrical conductivity has long been studied in glass-forming molten salts and polymers,[8,9] and recently in some aluminosilicate melts,[10,11] but there is a lack of investigation over a wide range of temperatures and compositions in borosilicate systems. Exceptions include an electrical conductivity study of a multicomponent borosilicate glass[12] and three SBN glasses with an Na_2O/B_2O_3 ratio of less than 0.5.[13] Both these studies were carried out over a small temperature range (from 1000 to 1200 °C and from 600 to 900 °C, respectively).

This paper compares the viscosity and electrical conductivity measurements in the simple sodium-borosilicate system. The results are discussed in terms of structural behavior at high temperature, using NMR results from the literature[14] and a Raman spectroscopy analysis performed at different temperatures. The transport properties of the molten state and of the glassy state are also compared, using ionic conductivity measurements previously published,[15] T_g data, and ^{11}B NMR data[16,17] obtained in the glassy state near T_g.

II. EXPERIMENT

A. Glass preparation

The fabrication of SBN glass samples and the glass transition temperature measurements have already been explained in detail elsewhere.[15] The SBNx composition is nevertheless indicated in Table I.

B. Electrical conductivity measurements

Electrical conductivity measurements in the molten state were performed by impedance spectroscopy using a four-probe electrode cell. The setup for those measurements is described in detail elsewhere.[18] The platinum electrodes were immersed in the melt at a temperature for which the viscosity is sufficiently low (about 30 dPa s) to avoid electrode bending or damage. The conductivity was measured in 10 °C steps from the upper limit of the temperature range (which depended on the melt composition) to $T_g - 100$ °C by applying a cooling rate of 120 °C per hour. The four-probe cell was calibrated using aqueous KCl solutions with a room-temperature electrical conductivity close to that of the molten oxide studied.

C. Viscosity measurements

The viscosity of the six glass compositions (SBN12–SBN35) was measured by a rotating cylinder method using a Couette-type apparatus; the melt was contained in a

TABLE I. Composition and properties of SBN glass samples studied (B^{IV}=four-coordinated B).

Glass	SBN12	SBN15	SBN20	SBN25	SBN30	SBN35
Composition (mol %)						
SiO_2	59.66	57.63	54.19	50.76	47.33	43.95
B_2O_3	28.14	27.13	25.51	23.89	22.28	20.63
Na_2O	12.20	15.24	20.30	25.35	30.39	35.42
B^{IV} calc.[a]	0.43	0.56	0.62	0.60	0.57	0.54
m [Eq. (6)] (±0.01)	0.43	0.42	0.39	0.34	0.39	0.39
T_g (K) from DTA (±5 K)	816	824	838	808	767	740
T_{0vft} (K)						
From conductivity	419	441	543	528	487	450
From viscosity	677	702	802	759	758	711
E_{VFT} (eV)						
From conductivity	0.42	0.37	0.24	0.22	0.20	0.20
From viscosity	0.49	0.45	0.28	0.27	0.23	0.22
Preexponential factor						
σ_{0vft} (S/cm)	12.7	13.1	7.3	7.8	11.0	14.6
η_{0vft} (dPa s)	0.031	0.033	0.093	0.0686	0.1028	0.0895

[a]Reference 16.

29-mm-diam Pt/10% Rh crucible, and a 14-mm-diam spindle was suspended from the rheometer and immersed in the melt. The rheometer (Lamy Rheomat 115) rotated the spindle and measured the torque induced by the viscosity of the liquid. The whole system was calibrated with the NBS717 (National Bureau of Standards No. 717) standard glass.

The viscosity of a fluid is defined as the ratio of shear stress to shear rate. The glass sample was heated in the crucible to about 1200 °C, depending on the composition, and the spindle was then immersed in the melt. The sample temperature was maintained and the shear stress was measured as a function of the rotational speed. The sample temperature was then decreased in 25 or 50 °C intervals. The viscosities were measured again during the reheating of the melt, to ensure that no significant volatilization had occurred or that the system variables had not drifted from their initial values.

D. Micro-Raman analysis

Unpolarized Raman spectra were measured on a Jobin-Yvon T64000 confocal micro-Raman spectrometer equipped with a charge-coupled-device (CCD) detector.[19] For high-temperature Raman analysis the glass sample was placed in a microheater similar to the "Mysen-Frantz cell."[20,21] This device, heated by the Joule effect, is constituted by a PtRh (10%) single-alloy wire. The temperature was calibrated against the melting points of several known compounds between 25 and 1500 °C.[20] The sample was held within a small hole (about 1 mm in diameter), where it remained even at $T > T_{melting}$ thanks to the surface tension. All spectra were recorded between 20 and 1200 cm^{-1} with a precision of ±1 cm^{-1} and corrected for temperature and frequency-dependent scattering intensity using the recommended factor.[19–21]

III. THEORETICAL MODELS

A. Transport properties

Dynamic properties Φ (such as the resistivity or viscosity of glass-forming melts) correspond to thermally activated processes. These macroscopic properties increase when the temperature decreases. If their activation energies were temperature independent, the experimental data should result in a straight line when plotted in Arrhenius coordinates. But for both electrical conductivity and viscosity, the experimental data do not follow an Arrhenius law. It is therefore generally assumed that these activation energies depend on the temperature. One of the best known expressions used to describe viscosity and resistivity experimental data is the empirical Vogel-Fulcher-Tammann (VFT) equation

$$\Phi = \Phi_0 \exp\left(\frac{B}{T - T_0}\right). \quad (1)$$

According to this equation, the property Φ (such as viscosity) diverges at temperatures approaching T_0.

The validity of this equation has been described by various theories, especially for the viscosity-temperature relationship.

Cohen and Grest[22] developed the free-volume model, which assumes that atoms are confined in cells defined by their nearest neighbors. With certain approximations this approach leads to Eq. (1). When the cell volume exceeds a critical value the excess volume, or "free volume," can be redistributed among the other cells. The cell volume fluctuations allow the atoms to diffuse. When this model is applied for viscosity data, T_0 represents the lowest temperature for which the free volume needed for a diffusive step can be formed.

The Adam-Gibbs model[23] is based on the idea that motion occurs by internal cooperative rearrangement of independent regions. When temperature decreases, the motion of one molecule disturbs an increasingly larger number of its neighbors. The authors assume that the increasing size of the subsystems when lowering the temperature reduces the probability of a transition between configurations and then introduces a temperature-dependent activationlike energy. Adam and Gibbs then found a correlation between the structural relaxation time of the glass-forming melt and the configurational entropy.

In most electrical conductivity measurements, where the VFT law is observed, a cooperative transport mechanism has been evidenced.[11,12,24,25] Thus the enhanced conductivity observed above the glass transition temperature could be explained by the fact that the network restructuring provides additional possibilities for the diffusion of mobile species.

Souquet and co-workers *et al.*[24,26] have proposed a general description of the ionic conductivity mechanisms in glass-forming oxides. They assumed that most of the alkali cations are associated with nonbridging oxygen. In their model, thermal vibrations allow partial dissociation, which leads to the formation of a "defect" in the glass structure, analogous to the formation of a Frenkel defect in an ionic crystal. This model assumes that, as for ionic crystals, cation displacements result from the migration of interstitial pairs dominated by an activated jump mechanism at low temperature and by a cooperative free-volume mechanism above T_g. For alkali silicates in the molten state the ionic conductivity is proportional to the alkali mobility, which depends on a physical correlation factor for subsequent jumps of the associated "defect" motion. Here defects are seen both from a structural (or spatial) and an energetic (or temporal) standpoint. This leads to the concept of "structured" glass melts. In glass melts with vanishing long-range order, at the atomic scale, the movement of ions still depends on the intermediate-range order and on necessary statistical fluctuations of energy barriers. In glass-forming melts, these different energy levels are less distinct than in a regular lattice. The "defects"' could then be defined as long as an intermediate range order persists—i.e., not only at $T < T_g$, but also at higher temperatures.[25]

B. Glass structure

The structure of glasses in the SiO_2-B_2O_3-Na_2O system has been well described and modeled by Yun and Bray[16] and Dell, Bray and Xiao[17] thanks to ^{11}B NMR experiments. The simplified model assumes that for the composition range $R \leq 0.5$, where $R = [Na_2O]/[B_2O_3]$ in mol%, the Na^+ ions are first attracted by the borate network as charge compensators. For $0.5 < R < R_{max}$ (where R_{max} depends on the ratio $K = [SiO_2]/[B_2O_3]$ in mol%), diborate groups are disassociated and recombine with all the existing SiO_2 to form reedmergnerite and danburite groups.[27,28] Then, when $R > R_{max}$, additional Na^+ are shared between the borate and silicate networks to form nonbridging oxygen (NBO). More recent publications reporting ^{11}B, ^{17}O, ^{23}Na, and ^{29}Si magic angle spinning (MAS) NMR and Raman studies on both molten
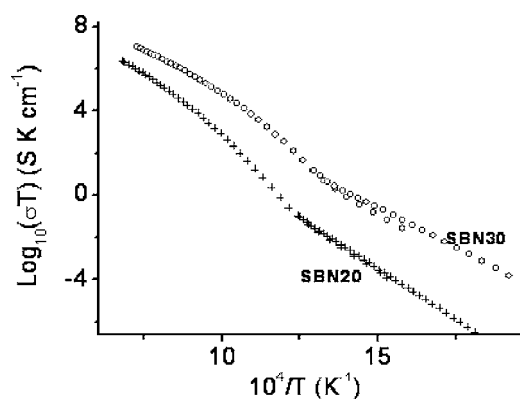
FIG. 1. Temperature dependence of electrical conductivity of SBN20 and SBN30 in their glassy and molten state.

and sol-gel prepared alkali borosilicate glasses have shown that in general alkali cations are more randomly mixed to the borate and silicate networks.[29,30] The model of Yun and Bray and Dell *et al.* is nonetheless useful for a visual description of the structure evolution as alkali cations are added to the composition. We have then applied this model to our samples: the B^{IV} fraction calculated for each composition is reported in Table I.

IV. RESULTS AND DISCUSSION

A. Electrical conductivity temperature dependence

The molten-state electrical conductivity measurements obtained by four-electrode impedance spectroscopy were validated by comparing the low-temperature data (around T_g) with data obtained using standard solid-state calibration-free measurements.[15] Data overlapping around T_g, are shown in Fig. 1 for two different compositions. The two different techniques provide comparable values in their common temperature range. The four-electrode method tends to underestimate the electrical conductivity when $T \lesssim T_g$. This slight discrepancy can be attributed to an increased cell constant due to shrinkage effects at low temperature and to different cooling and heating rates used for the two methods. In this study, we will take into account conductivity data only for temperatures higher than $T_g + 100$ K (see below).

Above T_g, the conductivity increases more rapidly than the Arrhenius law and tends toward VFT behavior:

$$\sigma = \sigma_0 \exp\left(-\frac{E_\sigma}{R(T - T_{0\sigma})}\right), \qquad (2)$$

where σ_0 is the preexponential factor and E_σ a pseudoactivation energy.

All the experimental data fitted with Eq. (2) are shown in Fig. 2, and the adjustable parameters for each composition are provided in Table I. All fits were performed within the temperature range from $T_g + 100$ K to $T_g + 570$ K.

B. Viscosity temperature dependence

The viscosity temperature dependence for the compositions listed in Table I is shown in Fig. 3. Newtonian flow was
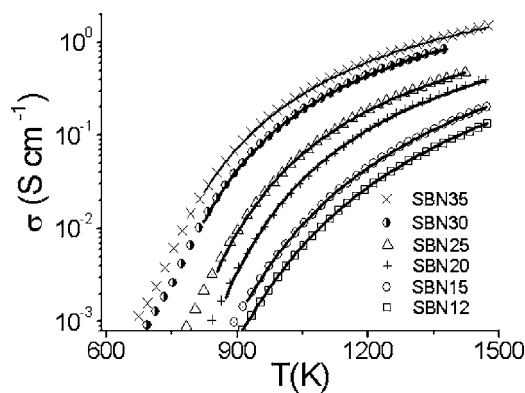
FIG. 2. σ experimental data (scatter) and VFT fits (see table I) (line) for all the compositions studied

observed for all melts; i.e., the shear stress to shear rate ratio was constant at each temperature. Deviations from the Arrhenius law are observed in the temperature range studied, for each sample. As described in Sec. III, these data can be fitted by the empirical VFT law

$$\eta = \eta_0 \exp\left(\frac{E_\eta}{R(T - T_{0\eta})}\right), \tag{3}$$

where η_0, the preexponential factor, E_η, a pseudoactivation energy, and $T_{0\eta}$, seen as the ideal glass transition temperature, are the three adjustable parameters. These parameters are studied for each composition and reported in Table I.

C. Viscosity and electrical conductivity composition dependence

The compositional dependence of the viscosity of a glass-forming melt is closely related to the connectivity of the structure.

Plots of $\log(\eta)$ versus $1/T$ for all compositions (Fig. 3) showed an increasing slope with decreasing temperature, indicating that the activation energy for viscous flow is a function of temperature and deviates from the simple Arrhenius relationship behavior.

We did not measure the viscosity in the glass transition range, but the transition temperature T_g measured by differ-
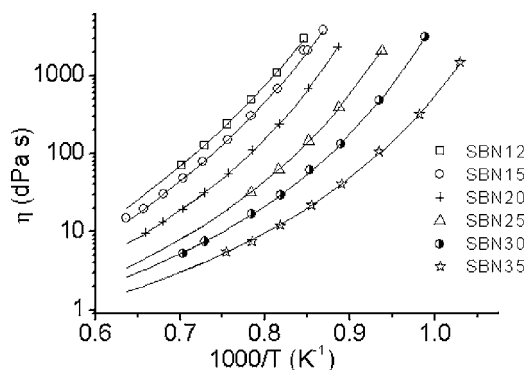
FIG. 3. Experimental data (scatter) and VFT fits (line) of viscosity $\text{Log}(\eta)$ (viscosity in dPa·s) versus $1000/T$ for the SBN melts.
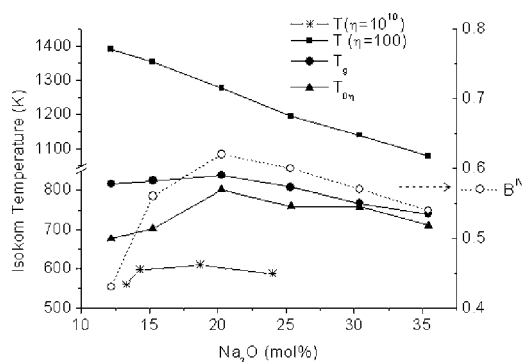
FIG. 4. Isokom temperature at $\eta = 100$ dPa·s (full squares), T_g measured by ATD (full circles), $T_{0\eta}$ obtained from the VFT law (full triangles), compared with the fraction of B^{IV} calculated thanks to the moldel of Yun (hollow)[16] and isokom temperature at $\eta = 10^{10}$ dPa·s for borosilicate glasses with a SiO_2/B_2O_3 ratio near 2.12 measured by Akimov [6] (stars) as a function of the Na_2O content (mol%).

ential thermal analysis (DTA) and the ideal glass transition temperature $T_{0\eta}$ provide significant information about the flow behavior of the melt in this high-viscosity region.[31] Figure 4 shows the isokom temperature at $\eta = 100$ dPa s compared with T_g and $T_{0\eta}$ as a function of the Na_2O content. We have also indicated in this figure the B^{IV} fraction calculated by the Yun-Dell-Bray-Xiao model.[16,17] Akimov[6] measured the viscosity of glasses of the SiO_2-B_2O_3-Na_2O system in the glass transition region by the compression method as a function of the composition and temperature. We have indicated in Fig. 4 the isokom temperature at $\eta = 10^{10}$ dPa s obtained by Akimov for glasses of composition close to our samples—i.e., with an SiO_2/B_2O_3 ratio near 2.12. This figure shows clearly that in the glass transition region the compositional dependence of the viscosity is different from the one corresponding to the low-viscosity range. Indeed, at low temperatures, T_g, $T_{0\eta}$, and $T(\eta = 10^{10}$ dPa s) (Ref. 6) increase with the Na_2O content until R is about 0.8 (Na_2O close to 20 mol %) and then decrease with the Na_2O content. This result suggests that the changes in structural arrangement with the composition are different in the high- and low-viscosity ranges.

In the case of sodium-borosilicate glasses, as assumed by Dell, Bray, and Xiao for $R < R_{max}$, almost all the sodium ions are used in the creation of tetracoordinate boron regardless of the SiO_2 concentration. Therefore, for $R < R_{max}$, the addition of Na_2O to the silicate network strengthens the melt structure by modifying the elementary boron unit structure—i.e., replacing boroxol rings (B^{III} units) by B^{IV} species. For $R > R_{max}$, the excess sodium atoms form nonbridging oxygens by breaking the Si-O-Si or Si-O-B bonds and subsequently decrease the melt viscosity. This is consistent with the observations of Shiraishi *et al.* who also measured an effect of the change in the oxygen coordination number of the boron atom (from 4 to 3) on the viscosity of sodium borosilicate melts near the transition temperature.[7]

At high temperature, in the temperature range where the viscosity is below 10^4 Pa s, the melt $\log \eta$ decreases and $\log \sigma T$ increases—both linearly—with the Na_2O content, as
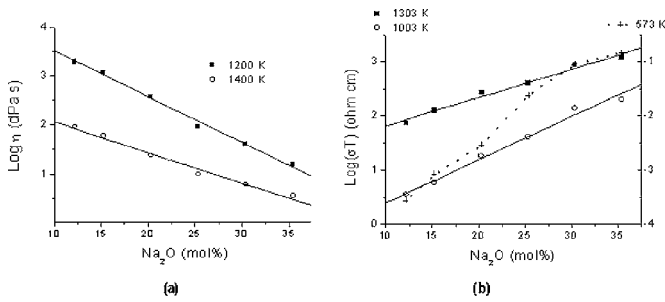
FIG. 5. a) isoviscosity at 1400 K and 1200 K as a function of the Na_2O content, b) isoconductivity in the liquid state at 1503 K and 1303 K and in the solid state [15] at 573 K as a function of the Na_2O content. Linear fits are provided (straight lines)

shown in Figs. 5(a) and 5(b). In this study, a linear variation with Na_2O mol % also implies a linear variation with B_2O_3 or SiO_2 mol % because the SiO_2/B_2O_3 ratio is constant at 2.12. This behavior is in agreement with published viscosity measurements in sodium-borosilicate melts.[2] The change of viscosity of a silicate melt with the temperature is associated with the frequency of the breaking and bridging of T-O bonds, where T stands for tetracoordinated cations.[32] Borosilicate liquids present a rich array of dynamic possibilities as their structural network contains both silicate and borate groups. Very few studies directly connect the liquid-state dynamics to specific structural mechanisms, so it is difficult to connect these transport measurements to a structural "dynamics." Recently, Stebbins and Sen studied dynamic processes in an alkali-borosilicate melt by high-temperature ^{11}B and ^{29}Si magic angle NMR spectroscopy.[14] They concluded that, in the melt studied, the controlled step in viscous flow is local network bond breaking and rearrangement of small structural units, involving boron and silicon. The NMR exchange rates indicate close coupling between B-O and Si-O bond breaking in the liquid state. Our results show that the number of B^{IV} structural units no longer influence the viscosity or the electrical conductivity in this temperature range. This result may be explained by high-temperature Raman spectra.

Raman spectra were recorded from room temperature to 1200 °C in samples SBN25 and SBN35. Figure 6 shows the comparison between the spectra obtained at room tempera-
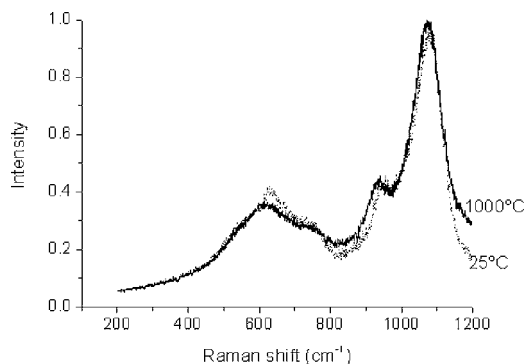
FIG. 6. Comparison between the spectrum recorded on a SBN35 glass sample at room temperature and the spectrum on the same specimen heated up to 1000 °C.

ture and at 1000 °C. The 630-cm^{-1} band can be attributed to the four-atom ring of SiO_4 and BO_4 of danburitelike structure and according to Bunker et al. is characteristic of borosilicate structures.[28] The presence of this danburite band at 630 cm^{-1} is a way to identify the borosilicates units.[28] The bands in the 700–800-cm^{-1} region could be attributed to borate rings containing both trigonal and tetrahedral boron.[33]

The effect of temperature and of sodium content on the Raman spectra will be discussed in more detail in a forthcoming paper. Figure 6 clearly shows that the intensity of the bands attributed to the borosilicate units (630 cm^{-1}) considerably decreases with temperature. The intensity of the bands in the 700–800-cm^{-1} range, attributed to borate rings, also decreases at 1000 °C compared to room temperature. After heating to 1200 °C and cooling to room temperature, we observe the reformation of these borosilicate units: indeed the intensities of the 630-cm^{-1} band and of the bands in the 700–800-cm^{-1} region are the same before and after this heating cycle. The intensity decrease of these spectral bands is related to the gradual disappearance of the B^{IV} units. This result is in agreement with the assumption made above to explain the viscosity and the conductivity behavior at high temperature.

D. Electrical conductivity versus viscosity

Viscous flow of liquid is strongly related to the structural relaxation time. Macroscopically, the increased relaxation time with decreasing temperature is due to the decreased configurationally entropy,[23] which is a bulk property. On the other hand, electrical conductivity is determined by the motion of network-modifier cations and especially below the glass transition point does not vary with the viscosity. Nevertheless, at high temperature these two properties are coupled as predicting by the Stokes-Einstein and Nerst-Einstein relations.

The fundamental Stokes-Einstein equation states that a diffusion coefficient D of a Brownian particle is inversely proportional to the shear viscosity η:

$$D = \frac{kT}{\eta(6\pi)r}, \qquad (4)$$

where r is the radius of the particle and k the Boltzmann constant. The meaning of this relationship is clearly related to the homogenous character of the strain of pure liquids: every atomic movement is coupled to external stresses and produces both diffusion and deformation.

Applying the Nernst-Einstein law, which binds the total conductivity of the melt to the diffusion coefficient for ionic liquids, yields a relation between the electrical conductivity and the viscosity of the melt irrespective of its composition:

$$\sigma T \propto D \propto \left(\frac{T}{\eta}\right). \qquad (5)$$

Relation (5) suggests a slope of 1 between σT and T/η in a log-log plot. Figure 7 shows such a plot for our experimental data up to the fabrication temperature. We observe a deviation from linearity, which could be well described assuming
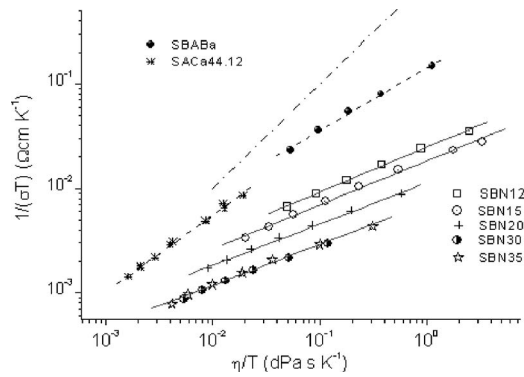
FIG. 7. $1/\sigma T$ as a function of η/T in log-log plot for all SBN12 to SBN35, SBABa glass and SACa44.12 and their linear fit. The dash dot line corresponds to the slope m equal to 1 (see equation (6)). Conductivity data of SACa44.12 are from ref. 10 and viscosity date of SACa44.12 from.[35]

a modified fractional Stokes-Einstein law, replacing Eq. (5) by

$$\sigma T \propto \left(\frac{T}{\eta}\right)^m. \qquad (6)$$

This relation with an average coefficient $m=0.39\pm0.05$ provides a satisfactory fit for all the sodium-borosilicate compositions studied. Moreover, the proportionally factor depends on the Na_2O content.

Figure 8 shows the variation of σ_t and $58(T/\eta)^{0.42}$ for SBN15 versus the inverse of the temperature over a large temperature range. Here, the low-temperature viscosity was obtained by extrapolating the experimental data according to the VFT equation and using the fit of the modified Stokes-Eintsein law for SBN15. As explained before, it appears that at low temperature the bulk (viscosity) and local transport (electrical conductivity) properties are decoupled, whereas at high temperature they are coupled.

A breakdown of the Stokes-Einstein viscosity-diffusion law has been observed in pure and mixed ionic melts.[9,34–36] Experimental data obtained by Voronel *et al.*[9] in ionic melts
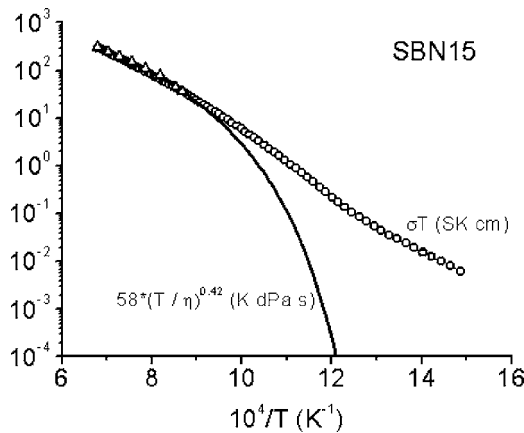
FIG. 8. σT (open circles) and $58(T/\eta)^{0.42}$ calculated (line) and experimental (open triangles) versus $10^4/T$ in log plot for SBN15. The value of 58 and m (0.42) were obtained from the fit of figure 7.

show a slope clearly less than 1 and close to 0.8. A coefficient $m \neq 1$ in Eq. (6) means that, although they are linked, the electrical conductivity and the viscosity have different temperature dependences: the liquid has a "structure."

Figure 7 also shows some results obtained on two melts without alkali cation: SBABa (48.8 SiO_2, 21.1 B_2O_3, 8.6 Al_2O_3, 20.1 BaO, 1.4 La_2O_3) and SACa44.12 (44 SiO_2, 12.5 Al_2O_3, 43.5 CaO) (compositions in mol %). The conductivity and viscosity data corresponding to the last melt come from the literature.[10,37] In these two cases of silicates without alkali cation, relation (6) fits well with a coefficient m larger than in the previous alkali glasses. The coefficient $m=0.6$ in the case of the borosilicate glass with Ba (SBABa) and $m=0.7$ in the case of the aluminosilicate glass with Ca (SACa44.12). This nonlinear character of the Stokes-Einstein law suggests a difference in elementary transport mechanisms, associated with the electrical conductivity, and the structural relaxation involved in viscous flow.[8,9]

To contribute to the conductivity, the charges must be successfully moved from one position to another. To achieve this goal without backward movements, an initial ion displacement must be followed by a rearrangement of its neighbors. This movement is described by the "short-term" dynamics of ions. To contribute to the macroscopic viscosity, however, the restructuring of the neighbors must result in a further change of the local configuration: this corresponds to the long-term dynamics. Singh *et al.*[38] explain the differences between the conductivity and the viscosity by a temperature-independent geometric factor relating the short-term and long-term phenomena.

The lower coefficient m of the sodium-borosilicate melts, compared to alkaline-earth melts, may be attributed to lower dependence between the sodium motion in the melt and the relaxation process than in case of alkaline-earth motion.

V. CONCLUSION

Six glass samples in the SiO_2-B_2O_3-Na_2O system were synthesized with a constant SiO_2/B_2O_3 ratio. The samples were characterized by DTA, and electrical conductivity and viscosity measurements were carried out in their molten state. Micro-Raman spectroscopy was performed on one sample, at room temperature and at 1200 °C. In the transition temperature range the conductivity, the transition temperature T_g, and the extrapolated viscosity depend on the specific structure of alkali-borosilicate glasses and especially on the boron coordination number. Contrary to the solid state, at high temperature in the range of our viscosity measurements, we showed that the Na_2O/B_2O_3 ratio is no longer the relevant parameter to account for the compositional dependence of the transport properties such as viscosity and electrical conductivity. This result is confirmed by Raman spectroscopy which suggests a modification of the borate network with increasing temperature.

Nevertheless, this does not mean that ion motions are no longer dependent on the local structure of the melt. Experimentally we observe a strong deviation from the Stokes-

Einstein law that could be a sign of the decoupling between the sodium mobility and the structural relaxation processes. In this experimental temperature range the conductivity is correlated to the short-term dynamics of the sodium ions, whereas the viscosity exhibits a further requirement described by a long-term rearrangement of the local structure.

*Corresponding author. Electronic address: agnes.grandjean@cea.fr

[1] M. J. Plodinec, Glass Technol. **41**, 186 (2000).

[2] J. C. Tait, D. L. Mandolesi, and H. E. C. Rummens, Phys. Chem. Glasses **25**, 100 (1984).

[3] T. Takamori and M. Tomozawa, J. Am. Ceram. Soc. **62**, 373 (1979).

[4] M. Tomozawa and S. Sridharan, J. Am. Ceram. Soc. **75**, 3103 (1992).

[5] E. Saad, N. L. Laberge, and X. Feng, Nucl. Technol. **86**, 66 (1989).

[6] V. V. Akimov, Fiz. Khim. Stekla **17**, 757 (1989).

[7] Y. Shiraishi, L. Gra'Na'Sy, Y. Waseda, and E. Matsubara, J. Non-Cryst. Solids **95&96**, 1031 (1987).

[8] C. A. Angell, Solid State Ionics **105**, 15 (1998).

[9] A. Voronel, E. Veliyulin, V. Sh. Machavariani, A. Kisliuk, and D. Quitmann, Phys. Rev. Lett. **80**, 2630 (1998).

[10] G. Gruener, D. DeSousa Meneses, P. Odier, and J. P. Loup, J. Non-Cryst. Solids **281**, 117 (2001).

[11] G. Gruener, P. Odier, D. DeSousa Meneses, P. Florian, and P. Richet, Phys. Rev. B **64**, 024206 (2001).

[12] S. S. Fu, Phys. Chem. Glasses **38**, 100 (1997).

[13] H. Wakabayashi, Phys. Chem. Glasses **30**, 51 (1989).

[14] J. F. Stebbins and S. Sen, J. Non-Cryst. Solids **224**, 80 (1998).

[15] A. Grandjean, M. Malki, and C. Simonnet, J. Non-Cryst. Solids **352**, 2731 (2006).

[16] Y. H. Yun and P. J. Bray, J. Non-Cryst. Solids **27**, 363 (1978).

[17] W. J. Dell, P. J. Bray, and S. Z. Xiao, J. Non-Cryst. Solids **58**, 1 (1983).

[18] C. Simonnet, J. Phalippou, M. Malki, and A. Grandjean, Rev. Sci. Instrum. **74**, 2805 (2003).

[19] D. A. Long, *Raman Spectroscopy* (Mc Graw-Hill, New York, 1977).

[20] D. R. Neuville and B. O. Mysen, Geochim. Cosmochim. Acta **60**, 1727 (1996).

[21] D. R. Neuville, Phys. Chem. Glasses **46**, 112 (2005).

[22] M. H. Cohen and G. S. Grest, Phys. Rev. B **20**, 1077 (1979).

[23] G. Adam and J. Gibbs, J. Chem. Phys. **43**, 139 (1965).

[24] J. L. Souquet, M. Levy, and M. Duclot, Solid State Ionics **70&71**, 337 (1994).

[25] T. Pfeiffer, Solid State Ionics **105**, 277 (1998).

[26] E. Caillot, M. J. Duclot, J. L. Souquet, and M. Levy, Phys. Chem. Glasses **35**, 22 (1994).

[27] N. Ollier, T. Charpentier, B. Boizot, G. Wallez, and D. Ghaleb, J. Non-Cryst. Solids **341**, 26 (2004).

[28] B. C. Bunker, D. R. Tallant, G. L. Turner, and R. J. Kirkpatrick, Phys. Chem. Glasses **31**, 30 (1990).

[29] G. El-Damrawi, W. Müller-Warmuth, H. Doweidar, and I. A. Gohar, J. Non-Cryst. Solids **146**, 137 (1992).

[30] R. Martens and W. Müller-Warmuth, J. Non-Cryst. Solids **265**, 167 (2000).

[31] A. Sipp and P. Richet, J. Non-Cryst. Solids **298**, 202 (2002).

[32] M. Solvang, Y. Z. Yue, S. L. Jensen, and D. B. Dingwell, J. Non-Cryst. Solids **336**, 179 (2004).

[33] B. N. Meera, A. K. Sood, N. Chandrabhas, and J. Ramakrishna, J. Non-Cryst. Solids **126**, 224 (1990).

[34] C. A. Angell, Science **267**, 1924 (1995).

[35] M. Videa and C. A. Angell, J. Phys. Chem. B **103**, 4185 (1999).

[36] C. T. Moynihan, J. Electrochem. Sci. Technol. **126**, 2144 (1979).

[37] G. Urbain, Y. Bottinga, and P. Richet, Geochim. Cosmochim. Acta **46**, 1061 (1982).

[38] P. Singh, R. D. Banhatti, and K. Funke, Phys. Chem. Chem. Phys. **7**, 1096 (2005).